DOI: https://doi.org/10.24425/amm.2024.149795

C.Y. TAN[1*], M.A.A. MOHD SALLEH[1], N. SAUD[1], M. NABIALEK[2], A. RYLSKI[3]

A NON-DESTRUCTIVE EVALUATION OF MICROSTRUCTURAL ANALYSIS IN Sn-Ag-Cu SOLDER JOINT BY SYNCHROTRON X-RAY RADIATION TOMOGRAPHY

This paper demonstrates a non-destructive technique to evaluate the internal microstructure in the Sn-Ag-Cu (SAC) solder joint through synchrotron X-ray radiation tomography. Synchrotron X-ray tomography is increasingly utilized for characterizing the internal microstructure of materials in 3D images. A 3D model is reconstructed from a set of 2D projection images taken from different angles and angular position during the sample rotation, thus it could provide a more comprehensive description of the microstructure of an alloy compared to 2D images. In this paper, it is successfully observed and evaluated the internal microstructure of a 900 μm solder joint sample. The key principles and methods of synchrotron X-ray tomography are briefly described. Examples of quantitative and qualitative assessments on the grain refinement effect of Mg addition to SAC35 solder joint are also presented in this paper.

Keywords: Synchrotron tomography; SPring-8; Solder joint; 3D microstructure

1. Introduction

The development, application, and widespread use of tomography of materials and structures has been tremendous growth in the material science industry [1-5]. Synchrotron X-ray radiation has high brightness, high flux, and high collimation characteristic, allowing it to generate higher brilliance than that of lab-based X-ray [6]. The lab-based X-ray is typically produced by bombarding the anode with fast-moving electrons, resulting in 30-150 kV X-rays energy. On other hand, synchrotron X-ray is generated by dedicated synchrotron particles. The charged electrons in the synchrotron are accelerated to extremely high speed in the booster ring, then are transferred to closed loop storage ring by strong magnets. Along the circulating path, specific bending magnets or insertion devices are inserted to cause the radial acceleration of the electrons, producing synchrotron radiation tangential to the ring. With the advanced technique, synchrotron X-ray can be produced up to 8 GeV energies at Super Photo Ring (SPring-8), Japan.

Synchrotron X-ray radiation tomography technique has been increasingly applied in the studies of materials science and engineering. It is a technique that can non-destructively detect and characterize the internal microstructure of the alloy [7]. The principle of synchrotron tomography is based on the generation of 2D X-ray images by directing an X-ray beam from synchrotron light source and passes through the sample [8]. Further, a charge-coupled device (CCD) detector receives a large number of radiographic images at various angular positions during 360° rotation of the sample. After that, these 2D X-ray images are then reconstructed using reconstruction algorithms and software. The filtered back-projection algorithm is a commonly used procedure for image reconstruction [9]. The field of view is initially cropped to reduce the file size for reconstructions.

There is a fast and exciting growth of research outputs and progress by tomography scientists, researchers and industries. This technique provides an insight into the internal microstructure of materials in 3D model without destructing the sample, with minimal sample preparation. Compared to the 2D images obtained by optical and scanning electron microscopy, which have been shown to misrepresent the statistics of 3D microstructure [10]. 3D visualization provides more reliable qualitative and quantitative outputs. For instance, spatial distribution, particle volume, morphology of the particles, defect distribution in a sample could be rendered and measured. These provide

1 UNIVERSITI MALAYSIA PERLIS, CENTRE OF EXCELLENT ON GEOPOLYMER AND GREEN TECHNOLOGY (CEGEOGTECH), 02600 PERLIS, MALAYSIA
2 CZESTOCHOWA UNIVERSITY OF TECHNOLOGY, DEPARTMENT OF PHYSICS, FACULTY OF PRODUCTION ENGINEERING AND MATERIALS TECHNOLOGY,42-200 CZESTOCHOWA, POLAND
3 LODZ UNIVERSITY OF TECHNOLOGY, INSTITUTE OF MATERIALS SCIENCE AND ENGINEERING, 90-924 LODZ, POLAND
* Corresponding author: chiying95@outlook.com

fundamental insight into microstructure, correlating to the mechanical performance.

It has been reported that the reliability of the solder joint is depending on the microstructure [11]. Hence, it is crucial to understand the internal microstructure of a solder joint for predicting the life span and reliability during its application. Many studies have conducted finite element (FE) models to predict the mechanical behavior of the solder joints [10]. However, there is still a certain gap between actual situation and stimulated situation, as many settings such as the size and distribution in the solder joints are randomly set [12]. Therefore, the synchrotron tomography plays a crucial role as it could provide more detailed information. Due to the fact of high brilliance and high coherency of monochromatized X-ray at Spring-8, it is possible to obtain high resolution, high spatial resolution, and high contrast in its projection images. Salleh et al. have reported that 29 keV X-rays energy generated by synchrotron radiation is sufficient to detect the contrast between Sn, Cu, and Cu_6Sn_5 due to their dissimilar densities [13].

High Cu-content in solder alloys suitable for high temperature application, such as in engine components and braking system [14-16]. However, the addition of Cu content in Sn-based solder alloy may lead to the formation of large and massive Cu_6Sn_5. Cu_6Sn_5 was reported that will undergo polymorphic transformation from monoclinic to hexagonal at temperature around 186°C, which may threaten the mechanical and reliability of solder joints [17-20]. Previous studies have shown that the addition of alloying element/reinforced with nano powder can refine and stabilize the Cu_6Sn_5 phase [21-24]. Therefore, this paper is aimed to demonstrate the ability of synchrotron techniques to be used to observe the grain refinement effect of Sn-3wt%Ag-5wt%Cu due to minor addition of Mg in BGA scale solder joint.

2. Methodology

Materials and sample preparation. The solder alloys used in this research are Sn-3wt%Ag-5wt%Cu (SAC35) and Sn-3wt%Ag-5wt%Cu-0.10wt%Mg (SAC35-0.10wt%Mg). The procedure for preparing the solder alloys was described elsewhere [14]. To prepare the BGA-scaled solder joint, the solder sheet was rolled into 0.054 mm and punched into a disc shaped with 3 mm diameter. The disc-shaped solder sheets were heated to form 900 µm solder balls, sieving is needed to ensure the homogeneity of the size of solder balls. Then, the solder ball was placed on the printed circuit board (PCB) Cu substrate with a little smear of rosin mildly activated (RMA) flux. The PCB was then reflowed under the reflow temperature: the maximum temperature 250°C for 60s and cooled at a rate of 0.33°C/s. The residual of the flux was subsequently cleaned using acetone.

Experiment setup, process, and image reconstruction. The synchrotron X-rays tomography was conducted at beamline BL20XU at the SPring-8 synchrotron radiation facility, Japan. During the experiment, a 900 µm solder joint was glued on a zirconia tube, as per Fig. 1(a). The experimental setup for the tomography test is shown in Fig. 1(b). Monochromatized X-rays with energy, 29 keV were used on a sample rotated at 4s/rotation. Beam energy selection for Sn-based alloy was described elsewhere [13]. The incident beam was adjusted to 5 mm in width and 3mm in height to obtain the transmission images. The transmission images were captured by beam monitor with a pixel size of 6.5 µm × 6.5 µm at a rate of 3 fps. The distance of the beam monitor was 0.5 m away from the solder joint sample. Reconstruction of transmission images was done using 250 projected images over 180° by convolution back-projection method. The selected reconstruction area was the near center of the solder joint specimen. The reconstructed images were further rendered using ImageJ software to noise filtering as well as normalization as to enhance the quality of the images. Using the reconstructed images, a quantitative analysis of the internal microstructure in the SAC35 and SAC3-0.10wt%Mg solder joints was performed.

3. Result and discussions

By using SEM, it was found that minor addition (0.10wt%) of Mg into SAC35 solder alloys significantly refined the primary Cu_6Sn_5 particles. Fig. 2(a) and (b) show the SEM micrographs of SAC35 and SAC35-0.10wt%Mg solder alloy under as-casted conditions respectively. The black particles as shown in Fig. 2 are the primary Cu_6Sn_5 particles. It can be seen that there are some long rod-like particles present in SAC35 solder alloy, whereas, in SAC35-0.10wt%Mg solder alloy, the primary Cu_6Sn_5 particles

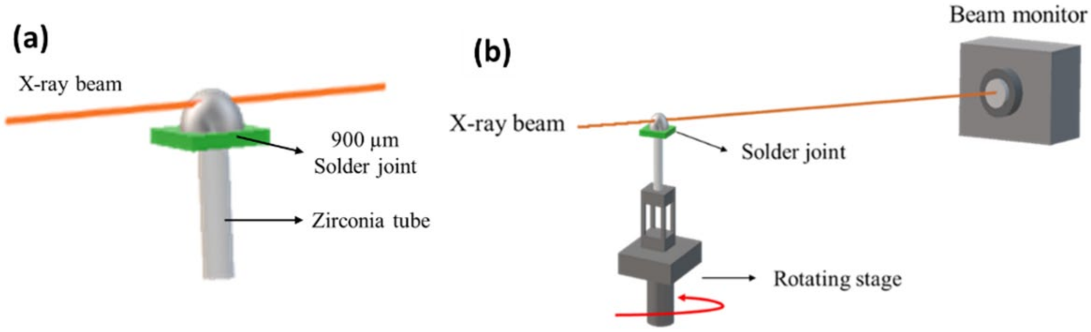

Fig. 1. (a) Sample set up: The alloy was soldered on a PCB substrate and placed on top of a zirconia tube then fixed on the rotating stage. (b) Schematics illustration of synchrotron X-rays tomography at BL20XU, SPring-8, Japan

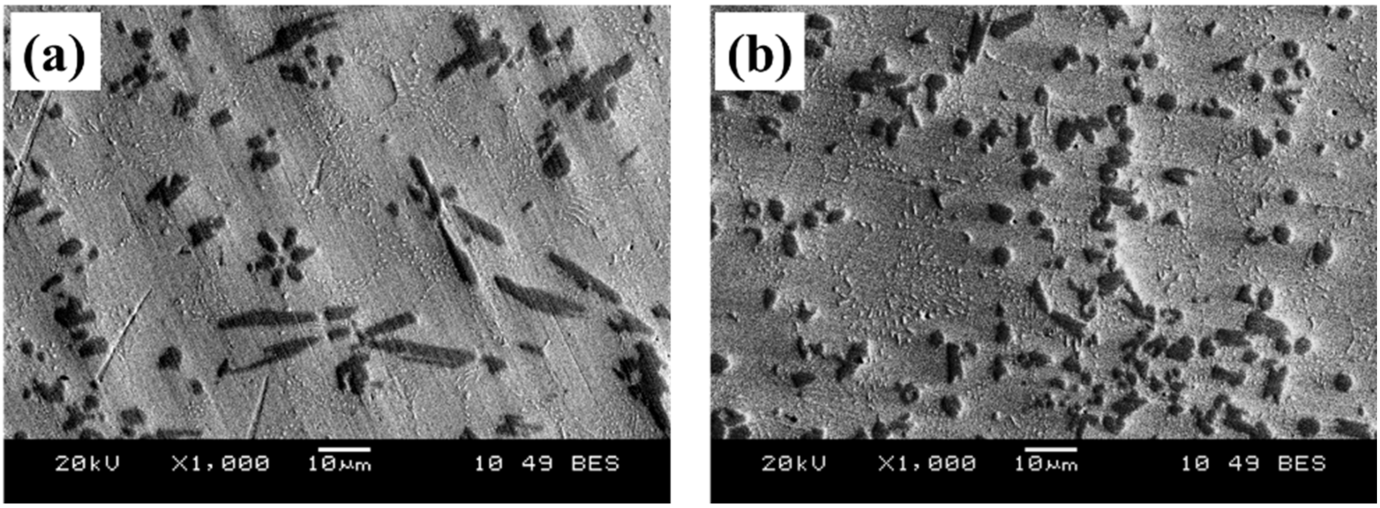

Fig. 2. SEM micrographs of (a) SAC35 and (b) SAC35-0.10wt%Mg solder alloys

are refined and shorter. A preliminary conclusion based on the 2D SEM micrographs is that the minor addition of MG could help to refine the primary Cu_6Sn_5 particles in SAC35 solder alloy. An in-depth study on the microstructural analysis was then conducted using synchrotron tomography technique.

Owing to high X-rays energy at BL20XU in SPring-8, it is sufficient contrast and resolution to observe the primary intermetallic compounds (IMCs) in the BGA-scaled SAC35-xMg solder joint. Fig. 3(a) shows the 3D reconstructed images at the near center of SAC35, and Fig. 3(b) represents SAC35-0.10wt%Mg solder joints under as-reflowed conditions. The green particles represent the primary IMCs that formed in the solder joints. The quantitative measurements were executed to calculate the number and mean volume of Cu_6Sn_5 particles in the selected area. There was approximately a total of 660 Cu_6Sn_5 particles were found in SAC35 sample (Fig. 2a), whereas it reduces to about 170 Cu_6Sn_5 particles with 0.10wt% Mg added to SAC35 (Fig. 2b). However, the minimum volume that can be traced by this technique is set to 10 μm^3. Therefore, it is believed that some diminutive Cu_6Sn_5 particles are untraceable in SAC35-0.10wt%Mg solder alloy. Besides, the mean volume of Cu_6Sn_5 particles was also reduced by 25% with only 0.10wt% Mg addition.

In addition, it is also sufficient resolution to render and focus on a single IMC. This allows the observation of more details on the morphology and shape of the IMCs formed. Fig. 4(a-e) reveals the morphology of primary IMCs that was found in the solder joint of SAC35 and SAC35-0.10wt% Mg. The primary IMC, typicall formed in SAC solder alloy, is identified as Cu_6Sn_5 and usually appears in a coarse and long-rod shaped morphology, which is nonoptimal for the reliability performance of a solder joint. It was found that the morphology of the primary Cu_6Sn_5 particles was become shorter and rounder after the presence of 0.10wt% of Mg addition, as per Fig. 4(d&e). Therefore, a clearer observation of the morphology of the primary IMCs allows the researchers to have better predictions of the mechanical properties and the failure mechanism is possible to be predicted.

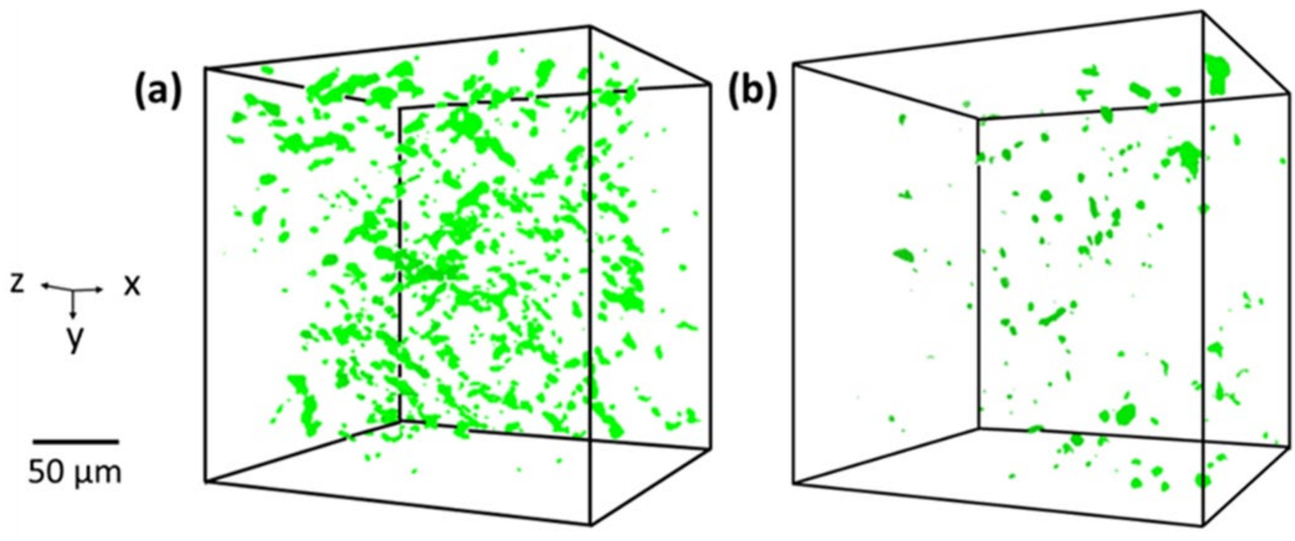

Fig. 3. Comparison of internal IMCs in the solder joint of (a) SAC35 and (b) SAC35-0.10Mg. Green particles are representing the primary Cu_6Sn_5 particles that formed in the solder joints

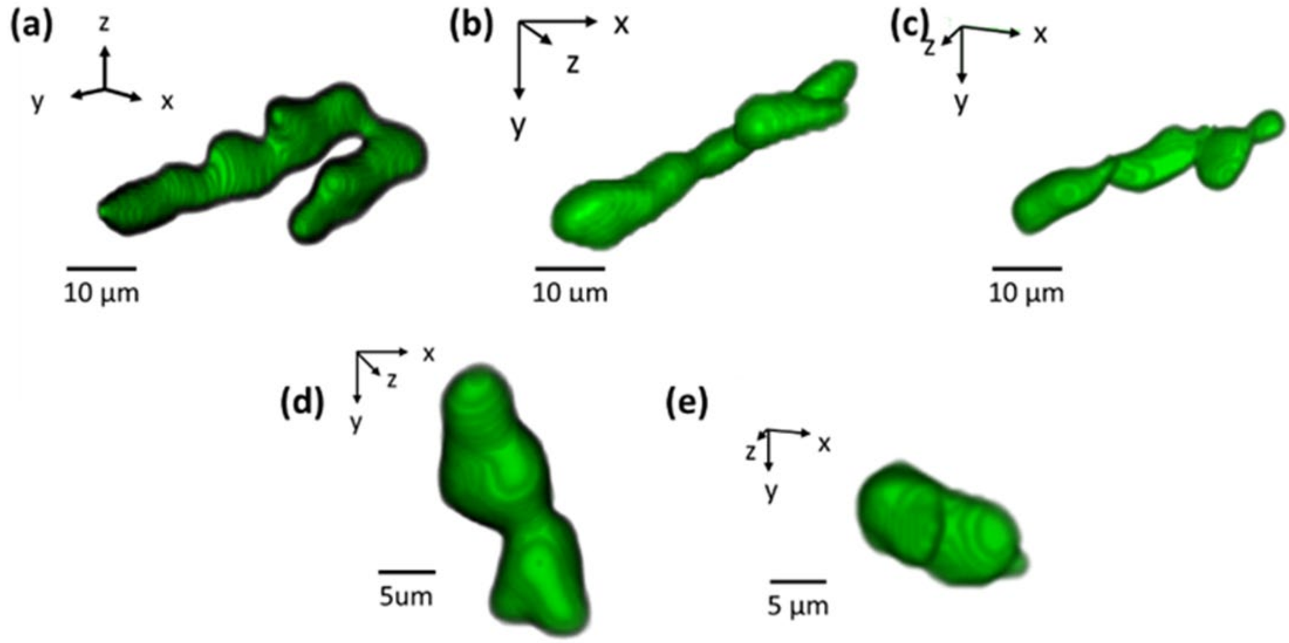

Fig. 4. 3D rendering on primary Cu_6Sn_5 found in (a-c) C and (d&e) SAC35-0.10wt%Mg solder joint

4. Conclusion

This experiment was successful and had sufficient contrast to differentiate primary Cu_6Sn_5 and matrix β-Sn phases. The experiment results show the ability of Mg to refine SAC35 alloy in 900 μm solder joint. This paper highlighted the potential of the use of the synchrotron X-ray tomography technique on the microstructural analysis on BGA scaled solder joint samples. This experiment was performed to evaluate the feasibility of using high energy (29 keV) synchrotron X-rays tomography technique to observe and measure the internal microstructure of primary Cu_6Sn_5 in the SAC35 solder alloys. Based on the results obtained, it is sufficient to observe the grain refinement on SAC35 solder alloy due to the addition of 0.10 wt% Mg.

Acknowledgements

The authors would like to gratefully thank the Universiti Malaysia Perlis (UniMAP)-Nihon Superior Ltd Co. collaboration research project and Fundamental Research Grant Scheme (FRGS) by Malaysia's Ministry of Higher Education for the financial support (Ref: FRGS/1/2020/TK0/UNIMAP/02/48). Many thanks to Dr. Kentaro Uesugi, Prof. Hideyuki Yasuda and his research team for technical supports at BL20XU of Spring-8. The contributions of Assoc. Prof. Mohd Arif Anuar Mohd Salleh and Prof. Kazuhiro Nogita to guidance and consultants to this paper are gratefully acknowledged.

REFERENCES

[1] B. Cai, J.Wang, A. Kao, K. Pericleous, A.B. Phillion, R.C. Atwood, P.D. Lee, 4D synchrotron X-ray tomographic quantification of the transition from cellular to dendrite growth during directional solidification. Acta Materialia **117**, 160-169(2016). DOI: https://doi.org/10.1016/j.actamat.2016.07.002

[2] W. Lin, B. Zhou, Y. Liu, X.Guo, T. Zheng, Y. Zhong, Q. Wang, Dendrite morphology in Al-20wt.% Cu hypoeutectic alloys in 24 tesla high magnetic field quantified by ex-situ X-ray tomography. Journal of Alloys and Compounds, 165679. (2022). DOI: https://doi.org/10.1016/j.jallcom.2022.165679

[3] Z. Song, O.V. Magdysyuk, T. Sparks, Y.-L. Chiu, B. Cai, Revealing growth mechanisms of faceted Al2Cu intermetallic compounds via high-speed Synchrotron X-ray tomography, Acta Materialia **231**, 117903 (2022). DOI: https://doi.org/10.1016/j.actamat.2022.117903

[4] Z. Zhang, C. Wang, B. Koe, C.M. Schlepütz, S. Irvine, J. Mi, Synchrotron X-ray imaging and ultrafast tomography in situ study of the fragmentation and growth dynamics of dendritic microstructures in solidification under ultrasound, Acta Materialia 209, 116796 (2021). DOI: https://doi.org/10.1016/j.actamat.2021.116796

[5] H. Yasuda, T. Kawarasaki, Y. Tomiyori, Y. Kato, K. Morishita, Characterization of dendritic growth in Fe–C system using time-resolved X-ray tomography and physics-based filtering. In IOP Conference Series: Materials Science and Engineering **529**, 1, 012023 (2019). IOP Publishing. DOI: https://doi.org/10.1088/1757-899X/529/1/012023

[6] A. Bharti, N. Goyal, Fundamental of Synchrotron Radiations. In Synchrotron Radiation-Useful and Interesting Applications: InTechOpen, (2019). DOI: https://doi.org/10.5772/intechopen.82202

[7] Z. Ding, N. Zhang, L. Yu, W. Lu, J. Li, Q.D. Hu, Recent Progress in Metallurgical Bonding Mechanisms at the Liquid/Solid Interface of Dissimilar Metals Investigated via in situ X-ray Imaging Technologies. Acta Metallurgica Sinica (English Letters): DOI: https://doi.org/10.1007/s40195-021-01193-6

[8] Y. Wang, S.C. Garcea, P.J. Withers, 7.6 Computed Tomography of Composites, in Comprehensive Composite Materials II, P.W.R. Beaumont and C.H. Zweben, Eds. Oxford: Elsevier 101-118. (2018). DOI: https://doi.org/10.1016/j.compscitech.2017.10.023

[9] K. Naresh, K.A. Khan, R. Umer, W.J. Cantwell, The use of X-ray computed tomography for design and process modeling of aerospace composites: A review. Materials & Design **190**, 108553 (2020).
DOI: https://doi.org/10.1016/j.matdes.2020.108553

[10] K.E. Yazzie, J.J. Williams, N.C. Phillips, F. De Carlo, N. Chawla, Multiscale microstructural characterization of Sn-rich alloys by three dimensional (3D) X-ray synchrotron tomography and focused ion beam (FIB) tomography. Materials Characterization **70**, 33-41 (2012).
DOI: https://doi.org/10.1016/j.matchar.2012.05.004

[11] M. Sona, K.N. Prabhu, Review on microstructure evolution in Sn–Ag–Cu solders and its effect on mechanical integrity of solder joints. Journal of Materials Science: Materials in Electronics **24**, 3149-3169 (2013).
DOI: https://doi.org/10.1007/s10854-013-1240-0

[12] S. Zhang, Z. Wang, J. Wang, G. Duan, H. Li, Study on the Influence of Defects on Fracture Mechanical Behavior of Cu/SAC305/Cu Solder Joint. Materials **15** (14), 4756(2022).
DOI: https://doi.org/10.3390/ma15144756

[13] M.A.A. Mohd Salleh, A. Sugiyama, H. Yasuda, S. McDonald, K. Nogita, In Situ Soldering Process Technique by Synchrotron X-Ray Imaging. Applied Mechanics and Materials **754-755**, 508-512 (2015). DOI: https://doi.org/10.4028/www.scientific.net/AMM.754-755.508

[14] C.Y.Tan, M.M. Salleh, X.F. Tan, H. Yasuda, N. Saud, M.I.I. Ramli, K. Nogita, Properties of Sn-3 wt% Ag-5 wt% Cu alloys with Cu6Sn5 intermetallics grain refined by Mg. Materials Today Communications **31**, 103221 (2022).
DOI: https://doi.org/10.1016/j.mtcomm.2022.103221

[15] S.A. Musa, M.A.A. Mohd Salleh, N. Saud, Zn-Sn Based High Temperature Solder – A Short Review. Advanced Materials Research **795**, 518-521 (2013).
DOI: https://doi.org/10.4028/www.scientific.net/AMR.795.518

[16] S. McDonald, K. Nogita, J. Read, T. Ventura, T. Nishimura, Influence of composition on the morphology of primary Cu6Sn5 in Sn-4Cu alloys. Journal of Electronic Materials **42** (2), 256-262 (2013). DOI: https://doi.org/10.1007/s11664-012-2222-3

[17] G. Zeng, S.D. McDonald, D. Mu, Y. Terada, H. Yasuda, Q. Gu, M.M. Salleh, K. Nogita, The influence of ageing on the stabilisation of interfacial (Cu, Ni) 6 (Sn, Zn) 5 and (Cu, Au, Ni) 6Sn5 intermetallics in Pb-free Ball Grid Array (BGA) solder joints. Journal of Alloys and Compounds **685**, 471-482. (2016).
DOI: https://doi.org/10.1016/j.jallcom.2016.05.263

[18] F. Somidin, H. Maeno, X.Q. Tran, S.D. McDonald, M.A.A. Mohd Salleh, S. Matsumura, K. Nogita, Imaging the polymorphic transformation in a single Cu6Sn5 grain in a solder joint. Materials **11** (11), 2229 (2018).
DOI: https://doi.org/10.3390/ma11112229

[19] F. Somidin, H. Maeno, M.M. Salleh, X.Q. Tran, S.D. McDonald, S. Matsumura, K. Nogita, Characterising the polymorphic phase transformation at a localised point on a Cu6Sn5 grain. Materials Characterization **138**, 113-119 (2018).
DOI: https://doi.org/10.1016/j.matchar.2018.02.006

[20] K. Nogita, M.A.A. Mohd Salleh, E. Tanaka, G. Zeng, S.D. McDonald, S. Matsumura, In situ TEM observations of Cu6Sn5 polymorphic transformations in reaction layers between Sn-0.7 Cu solders and Cu substrates. Jom, **68** (11), 2871-2878 (2016).
DOI: https://doi.org/10.1007/s11837-016-2020-0

[21] M.I.I. Ramli, M.M. Salleh, H. Yasuda, J. Chaiprapa, K. Nogita, The effect of Bi on the microstructure, electrical, wettability and mechanical properties of Sn-0.7 Cu-0.05 Ni alloys for high strength soldering. Materials & Design **186**, 108281 (2020).
DOI: https://doi.org/10.1016/j.matdes.2019.108281

[22] M.M. Salleh, S.D. McDonald, Y. Terada, H. Yasuda, K. Nogita, Development of a microwave sintered TiO2 reinforced Sn–0.7 wt% Cu–0.05 wt% Ni alloy. Materials & Design **82**, 136-147(2015).
DOI: https://doi.org/10.1016/j.matdes.2015.05.077

[23] J.W. Xian, M.A.A. Mohd Salleh, S.A. Belyakov, T.C. Su, G. Zeng, K. Nogita, H. Yasuda, C.M. Gourlay. Influence of Ni on the refinement and twinning of primary Cu6Sn5 in Sn-0.7 Cu-0.05 Ni. Intermetallics **102**, 34-45 (2018).
DOI: https://doi.org/10.1016/j.intermet.2018.08.002

[24] M.A.A. Mohd Salleh, M.H. Hazizi, Z.A. Ahmad, K. Hussin, K.R. Ahmad, Wettability, Electrical and Mechanical Properties of 99.3Sn-0.7Cu/Si3N4 Novel Lead-Free Nanocomposite Solder. Advanced Materials Research **227**, 106-111 (2011).
DOI: https://doi.org/10.4028/www.scientific.net/AMR.277.106